Prediction of Diaphragm Wall Deflection by Using Different Models for Deep Excavation in Sands

Mohd Sheob, M. Danish, and Md Asad Ahmad

Abstract The purpose of this investigation is to assess and contrast findings from analyses of deep excavations in an undrained condition using the most used three soil models. In this research, three distinct soil models were employed to predict the ground surface settlement and diaphragm wall deflection for deep excavation in sands. These models included the Mohr–Coulomb model (MC model), the hardening soil model (HS model), and the hardening soil small strain model (HSS model). A case study of a deep excavation that actually takes place in layers upon layers of sand in Kaohsiung city, Taiwan, and had well-documented monitoring data is employed for the analysis in this study, and soil investigation results compiled for the construction project served as the basis for selecting the geotechnical parameters. The results show that the wall deflections predicted by the Hardening soil with small strain model are relatively close to those results, which were derived from field measurements. The hardening soil model produces superior results, when compared to the Mohr–Coulomb model. The ground settlement results predicted by any of the three soil models were poor. To anticipate the wall deflection and compare the results of the 2D analysis, a 3D analysis in PLAXIS was also carried out in this study, and the outcomes of the 3D analyses were nearly identical below the excavated depth to those of the 2D analyses. This research shows that HS and HSS models in numerical calculations are useful for predicting the soil behaviour during excavation, and researchers and engineers can use the findings of this work to improve the accuracy of their numerical studies using constitutive soil models.

Keywords Deep excavation · Mohr–Coulomb model · Numerical modelling · Surface settlement · Hardening soil small strain model · Wall deflection

M. Sheob (✉) · M. Asad Ahmad
Department of Civil and Construction Engineering, National Taiwan University of Science and Technology, Taipei, Taiwan
e-mail: mohdsheobamu@gmail.com

M. Danish
Department of Civil Engineering, Aligarh Muslim University, Aligarh, India

K. R. Reddy et al. (eds.), *Recent Advances in Civil Engineering*, Lecture Notes in Civil Engineering 398, https://doi.org/10.1007/978-981-99-6229-7_6

1 Introduction

Densely populated urban and suburban areas necessitate frequent deep excavations for the construction of tall buildings, MRT systems, road tunnels, among many other facilities. When working in soft ground, deep excavation might cause unfavourable ground deformations that may compromise nearby buildings. Therefore, it is essential to foresee these shifts so that some safety measures can be implemented to lessen the effects of the ground deformation [1]. Many studies have explored the diaphragm wall and ground movements caused by deep excavations with different models [2–6]. However, the proper selection of the constitutive model for the soil, which has a direct impact on the design, has not been thoroughly examined in 2D and 3D simulation on FEM-based software, and this issue is investigated in present study; the selected models are MC model, the HS model, and the HSS model due its widely acceptability and consideration of unloading effect in simulation. Some researchers have developed empirical approaches to estimate the settlement amplitude and profile by using feedback from a number of historically well-documented excavations [6]. With PLAXIS, more settlement and lateral deformation were computed than had been determined by local surveys [7]. The study, which was based on the measured data gathered from 296 case histories, provided support for earlier research by showing that the stiffness of the retaining system has no effect on the deformations in non-cohesive soil or stiff clay, while in soft clay, there is a low correlation between the stiffness and wall deflections [8]. The maximum surface settlement caused by excavation ranges from 0.1 to 0.35% of H_e (depth of excavation), and the maximum surface settlement is located between 0.33 and 0.5 H_e from the margin of the excavation [9].

As the safety of nearby structures must always be taken into account, there is still a lot of work to be done to improve the accuracy of finite element analysis in urban excavation design. Accuracy is determined by the formulation of the model, and parameters. Some of the most widely applied constitutive models are linear and nonlinear stress–strain models, which have emerged over the past five decades [10–13]. Predicting movements caused by deep excavations by using numerical calculations is still difficult. Numerous choices, including boundary condition, comprehensibility of geometry, constitutive models, input parameters, and mesh generation; affect the precision of a numerical analysis. Soil input parameters can be determined through experimentation in the lab or in the field, or they can be calculated using empirical equations. Engineers' familiarity with numerical methods and soil constitutive models is crucial for accurate results from numerical analysis [14].

This research aims to evaluate the efficacy of three soil models in PLAXIS software to anticipating the actions, generated by a deep excavation in sands. The numerical calculations in this scrutiny are based on a case study of deep excavation that has been thoroughly documented in Kaohsiung city, Taiwan.

2 Case Study Overview

In this study, numerical assessments are based on a case study of Kaohsiung city, Taiwan. Culture Center Station, of MRT system in Kaohsiung, was closed by the construction site. The location was about 3 km east of Kaohsiung bay, in the middle of Kaohsiung city. The site was in rectangular shape with dimension of 70 m by 20 m. Diaphragm walls, that were used to contain the excavation while it was being excavated by the bottom-up technique of excavation, were 0.9 m thick, and height was 32 m; excavation took place over the course of five phases, with the deepest reaching 16.8 m; Table 1 outlines the stages of the construction process. Steel struts were used to support the retaining wall at four different heights, with an average horizontal distance of 5.5 m between each pair of struts. Figure 1 exhibits the cross section of site and existing ground condition. Figure 1 shows that the three clay layers (CL type) have negligible effects on excavation behaviour since they are so thin. The site excavation thus represents a prototypical instance of a deep excavation in sand, all of the soil parameters were obtained from a study that had previously analysed the wall deflection and settlement using a two-dimensional analysis [14]. The additional parameters required have been calculated by the given equations in each subsection. On the other hand, the purpose of this investigation is to contrast the findings obtained from 2D analysis with those obtained from 3D analysis.

Table 1 Excavation process of site

Excavation activities	Stage
Dewatering till 3.5 m	1
Excavated to the depth of 2.5 m below the GL	
Install first struts H400 × 400 × 13 × 21 at the depth of 1.5 m below the GL. Preload of each strut is 900 kN	2
Dewatering till 8.3 m	
Excavated to the depth of 7.3 m below the GL	
Install second struts H400 × 400 × 13 × 21 at the depth of 6.3 m below the GL. Preload of each strut is 2000 kN	
Dewatering till 11.65 m	3
Excavated to the depth of 10.65 m below the GL	
Install third struts H400 × 400 × 13 × 21 at the depth of 9.65 m below the GL. Preload of each strut is 2800 kN	
Dewatering till 15 m	4
Excavated to the depth of 14 m below the GL	
Install fourth struts H400 × 400 × 13 × 21 at the depth of 13 m below the GL. Preload of each strut is 2800 kN	
Dewatering till 17.80 m	5
Excavated to the depth of 16.80 m below the GL	
Construct the base slab	

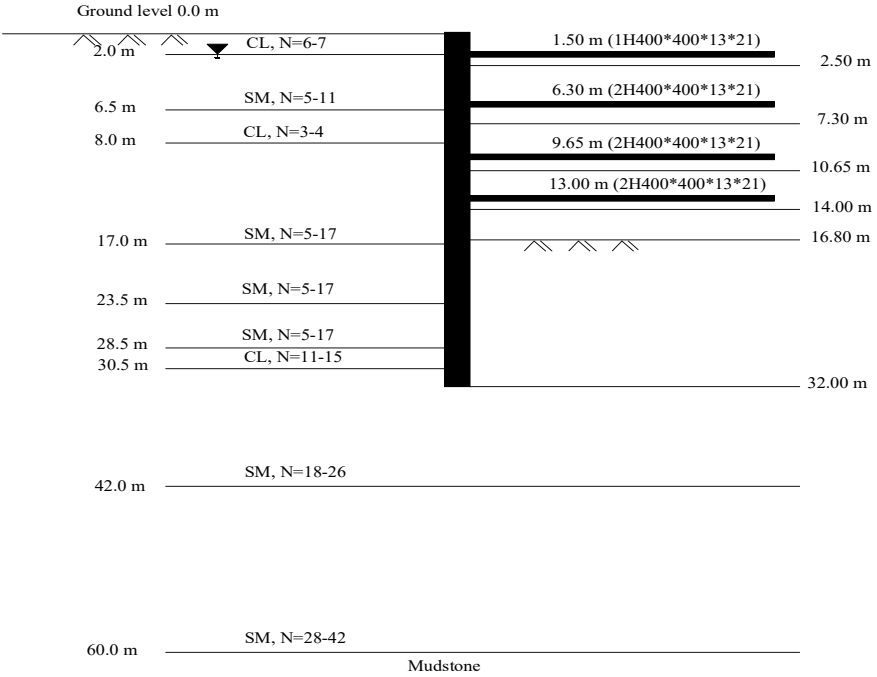

Fig. 1 Soil profile of excavation site

The reported groundwater level (GWL) before excavation was 2.0 m, and before the beginning of each phase of excavation, the GWL was nethered to a depth of 1 m below the planned excavation level to facilitate the work. Figure 1 describes the stratigraphic of site condition based on data gathered throughout the investigation: Clay (CL) makes up the initial layer to a depth of 2 m. It has an N value of somewhere between 6 and 7, which places it in the middle of the range for clay. The second layer, consisting of silty sand (SM) with N values of 5–11 and $\varphi\prime = 32°$ and a thickness of 2–6.5 m. Again, clay (CL) with an N value of about 3–4 makes up the third layer, which extends from 6.5 to 8 m deep. The fourth layer, from 8 to 17 m deep, consists of compact silty sand (SM) with an N value of 5–17, and $\varphi\prime = 32°$. The fifth layer consists of a medium-density silty sand (SM) that is from 17 to 23.5 m thick, with an N value of between 5 and 17, and $\varphi\prime = 32°$. Between 23.5 and 28.5 m deep, with a density of medium-to-dense silt sand and N value lies between 5 and 17 and $\varphi\prime = 33°$, lies the sixth layer. From 28.5 to 30.5 m beneath the sixth layer is more clayey soil, with N value of 11–15. Eighth layer properties are identical to those of the sixth layer from 30.5 to 42 m in depth, with N values of 18–26 and $\varphi\prime = 34°$. From 42 to 60 m down, a layer of compact silty sand (SM) with an N value of 28–42 and $\varphi\prime = 34°$.

The displacement of the ground and surrounding structures was observed by ground instrumentation. During the process of excavation, inclinometers had been

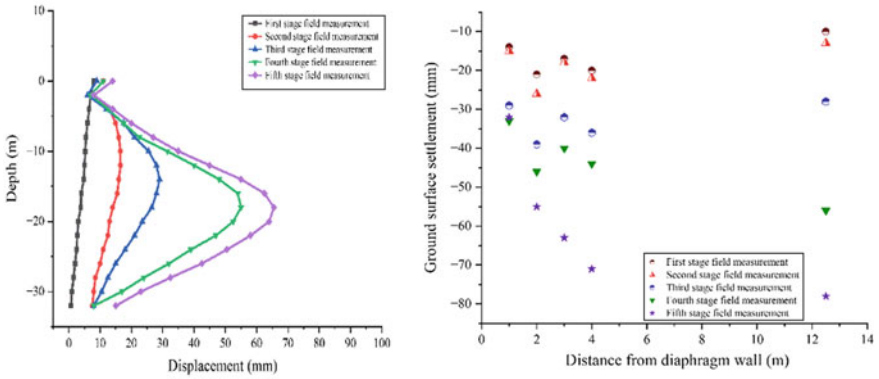

Fig. 2 Wall deflection and surface settlement by inclinometers and settlement observation instrumentation, respectively

used to monitor the wall deflections and settlement observation sections were used to monitor the surface settlements. In order to make sure that movements were acceptable, measurements acquired by the equipment were utilized to study the response of walls and nearby structures. They also contributed to provide the data that was used to support the accuracy of the numerical modelling in this research. Figure 2 depicts the actual wall deflections and ground surface settlements.

Figure 2 shows that during the first phase of excavation, the wall is meant to behave as a cantilever before the first-level steel struts have been erected and preloaded. Later excavation levels show the wall displaying deep inward shifts. At the end of excavation, the maximum value of wall deflection was reported as 0.39% of the total excavation depth (H_e). Consequently, this number agrees with the range of 0.2% H_e to 0.5% H_e discovered by a researcher [2]. It was difficult to see the entire extent of settlement beyond the retaining wall, because of the proximity of the excavation to the busy road. However, reported maximum values of surface settlement (δ_{vm}) in the end of excavation was around 0.125–0.1785% of H_e, or the ratio δ_{vm}/H_e is equivalent to 0.12–0.18%. Excavations in stiff clays and sands resulted in maximum surface settlements of around 0.15% of H_e [6].

3 Numerical Modelling

The evaluation software PLAXIS was employed in this study. The thin clay layers have no appreciable effect on excavation behaviour. As a counterexample, sand layers have a significant impact on excavation behaviour. In this work, three different soil models were used to replicate the sand layers in order to compare how well they predicted the surface settlements and wall deflections caused by the excavation of site. In the numerical computations, it was assumed that all sand layers included drained

materials. To ensure the consistent evaluation, a total stress undrained analysis of the clay strata was undertaken using the MC model; shear strength S_u, internal friction angle $\varphi_u = 0$, and undrained Young's modulus E_u were utilized for a total stress study of the clay layers in an undrained state. The empirical equation $E_u = 500\ S_u$ has been proposed to calculate the value of E_u [4, 5, 15]. The numerical difficulties associated with exceptionally low compressibility of water led to the adoption of Poisson's ratio $\nu_u = 0.495$ to model the behaviour of water. Clay layer input parameters utilized for analysis are listed in Table 2.

Plate element has been used in this study to simulate the diaphragm wall, while fixed-end anchor was used to simulate the steel struts; the steel struts and diaphragm walls were modelled using a linear elastic constitutive relationship. Young's modulus along with Poisson's ratio are the two input parameters needed for this model. The Poisson's ratio of steel struts and diaphragm wall was used as 0.2. The ACI Committee 318 (1995) formula was used to determine the diaphragm wall's Young's modulus:

$$E = 4700\sqrt{f_c}\ (\text{MPa})$$

In which f_c is the characteristic compressive strength of the concrete employed in the diaphragm walls. The Young's modulus of steel struts was considered to be 210 GPa. It is recommended to reduce the rigidity of the diaphragm wall by 30% and the steel struts by 40% from their standard values to account for cracks caused by bending forces in the diaphragm wall and to account for multiple uses and steel struts that were installed incorrectly, respectively [3]. The input parameters utilized in the numerical computations for the diaphragm wall are listed in Table 3 and for the steel strut are listed in Table 4.

Figure 3 shows the resulting numerical study of the site based on the finite element model. It was only necessary to reproduce half geometry of the site in order to excavate it because of its symmetry. The ideal distance between the lateral boundary

Table 2 Clayey soil parameters

Layer	Depth (m)	γ_t (kN/m^3)	S_u (kPa)	ν_u	E_u (kPa)
1	0.0–2.0	19.3	28	0.495	14,000
3	6.5–8.0	19.7	21	0.495	10,500
7	28.0–30.5	18.6	84	0.495	42,000

Table 3 Related parameters of diaphragm wall

Specifications	Value
Thickness Weight	0.9 m 4.95 kN/m/m
Axial stiffness 70%	15.66×10^6 kN/m
Poisson's ratio	0.2
Flexural stiffness 70%	1.057×10^6 kN-m^2/m

Table 4 Related parameters of steel struts

Strut level	Identification	Section area (m^2)	EA (kN)	Preload (kN)	60% EA (kN)
1	1H400 × 400 × 13 × 21	0.0219	4.59×10^6	900	2.75×10^6
2	2H400 × 400 × 13 × 21	0.0437	9.18×10^6	2000	5.50×10^6
3	3H400 × 400 × 13 × 21	0.0437	9.18×10^6	2800	5.50×10^6
4	4H400 × 400 × 13 × 21	0.0437	9.18×10^6	2800	5.50×10^6

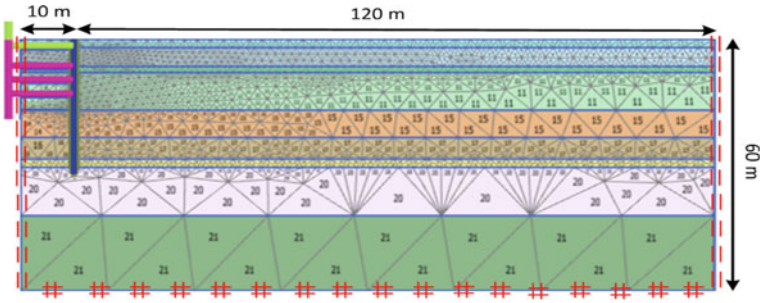

Fig. 3 Mesh used in this study

of the model and the diaphragm wall is seven times the depth of the excavation, i.e. 120 m [5]. The horizontal motion of model was restricted at its side boundaries. Vertical and horizontal mobility was limited at the bottom boundary of the model.

3.1 Mohr–Coulomb Model (MC Model)

In the field of geotechnical engineering, the MC model is commonly employed for the purpose of design because of its simplicity as a linear elastic-perfectly plastic model used to predict the material behaviour under monotonic loads. The relative simplicity of the model and necessity of only the most fundamental soil parameters, i.e. friction and dilation of soils, have made it a favourite among those interested in simulating the behaviour of soils. Sand layers were supposed to have zero effective cohesion (c') values; however, to keep PLAXIS calculations simple, layers of sand were assigned the extremely low value of $c' = 0.5$ kPa. Numerous studies assumed a drained Poisson's ratio of 0.3 for sand layers [5]. A study suggested the following method for determining the dilatancy angle for sands [16].

$$\text{If, } \Phi' \leq 30^\circ: \Psi' = 0, \text{ or } \Phi' > 30^\circ: \Psi' = \Phi' - 30^\circ.$$

The following formula, derived by a study, can be used to determine the coefficient of lateral earth pressure at rest.

$$K_0 = 1 - \sin \Phi'$$

The sand stiffness parameter E' is notoriously difficult to obtain an exact value from test results. This is because Φ' is closely associated with characteristics of the sand particles themselves, such as their surface roughness, compaction, and shape, all of which are seldom affected by the sample disturbance. Furthermore, the Young's modulus E' of sand is significantly affected by the sample disturbance since it is dependent on the physical qualities of sand and the intergranular force between the grains. Therefore, the E' is typically derived from empirical equations, this can be discovered through calibration studies of field-scale load testing or deep excavation case histories. In recent years, many geotechnical engineers now employ the standard penetration test (SPT) since it is reliable and inexpensive. As a result, several nations now routinely employ connections between SPT or N values and soil qualities. Scientists have proposed empirical links between the E' and N for sands in the form of $E' = A \times N$, where A is a correlation ratio [17]. This study similarly employed the following relation between E' and N: $E' = 2000N$ (kPa).

A researcher utilized an identical equation to describe the excavation of sands at the O6 station, located roughly 0.6 km from the actual excavation site [1].

3.2 Hardening Soil Model (HS Model)

A legitimate second-order model for soils is the HS model; the HS model uses the same failure criterion as the MC model and is a more sophisticated model. Before the primary loading reaches the fracture surface, the HS model uses the hyperbolic stress–strain relationship between vertical strain and deviatoric stress; plastic shear strain under deviatoric loading and cap hardening characteristics is modelled by using frictional hardening characteristics, while plastic volumetric strain under primary compression is modelled. Nine parameters are needed for the hardening soil model, i.e. three reference stiffness; triaxial unloading/reloading stiffness $E_{\text{ur}}^{\text{ref}}$, triaxial loading secant stiffness ref E_{50}^{ref}, and oedometer loading tangent stiffness $E_{\text{oed}}^{\text{ref}}$, along with a reference pressure p^{ref}, the value of p^{ref} typically taken to be 100 kPa (1 bar). The strain level to failure is determined by the failure ratio (R_{f}), the pure elastic Poisson's ratio or unloading/reloading Poisson's ratio (ν_{ur}); the Mohr–Coulomb strength parameters cohesion (c') and angle of internal friction (φ'); a power (m) for the stress-dependent stiffness; the fundamental one-dimensional compression K_0 value (K_0^{nc}). By using three reference stiffness, the HS model measures soil stiffness much more precisely.

$$\text{For sand } \boldsymbol{E}_{50} = \boldsymbol{E}_{50}^{\mathbf{ref}} \left(\frac{\boldsymbol{c'\cos\Phi\prime + \sigma_3\prime \sin\Phi\prime}}{\boldsymbol{c'\cos\Phi' + p^{ref}\sin\Phi\prime}} \right)^{\boldsymbol{m}} = \boldsymbol{E}_{50}^{\mathbf{ref}} \left(\frac{\boldsymbol{\sigma'_3}}{\boldsymbol{p^{ref}}} \right)^{\boldsymbol{m}}.$$

In which $\sigma_3\prime$ is the effective minor principal stress. The Mohr–Coulomb strength parameters and K_0 were identical to those in the MC model in every way. For sands, the values of m and ν_{ur} were set to 0.5 and 0.2, respectively [18]. As a default value in the PLAXIS, the R_f was taken to be 0.9. The E_{ur}^{ref} and E_{oed}^{ref} stiffness parameters were adjusted to $3E_{50}^{ref}$ and E_{50}^{ref} for sands, respectively. The back analysis between E_{50}^{ref} and N for the sand layers yielded the following best-fit relation [14].

$$E_{50}^{ref} = 1200N \text{ (kPa)}$$

3.3 Hardening Soil Small Strain Model (HSS Model)

The original hardening soil model has been improved with the hardening soil small strain (HSS) model, which consider the small strain properties of soil [19]. The HSS model comprises two extra parameters beyond the requirements for the hardening soil model, reference shear modulus at very low strain (G_0^{ref}) and the shear strain ($\gamma_{0.7}$) at which the secant shear modulus equals around 70% of its beginning value are the two additional parameters ($G_s = 0.722G_o = 0.722G_{max}$). The input parameters of HSS model were identical to those used in the HS model in every way. The PLAXIS user manual suggests the following equation to obtain the $\gamma_{0.7}$ value.

$$\gamma_{0.7} = \frac{1}{9G_0}\left[2c'\left(1 + \cos 2\varphi'\right) - \sigma_1\prime(1 + K_0)\sin 2\varphi'\right]$$

In which $\sigma_1\prime$ is effective vertical stress. The HSS model predicts far smaller wall deflections and surface settlements than those observed in the field when $\gamma_{0.7}$ was estimated according to the given equation, the estimation of $\gamma_{0.7}$ from above equation should be adjusted accordingly. However, the value of strain as 10^{-4} is typically considered to be a small strain. Consequently, $\gamma_{0.7}$ was assumed to be 10^{-4} instead of utilizing the above equation.

4 Results

4.1 MC Model

The sand layer input parameters of MC model are listed in Table 5.

Table 5 Sandy soil parameters of MC model

Layer	Depth (m)	Soil type	γ_t (kN/m^3)	N value	φ' (°)	c' (kPa)	E' (kPa)	ν'	ψ (°)	K_0
2	2.0–6.5	SM	20.9	5–11	32	0.5	16,000	0.3	2	0.47
4	8.0–17.0	SM	20.6	5–17	32	0.5	22,000	0.3	2	0.47
5	17.0–23.5	SM	18.6	5–17	32	0.5	22,000	0.3	2	0.47
6	23.5–28.5	SM	19.6	5–17	33	0.5	22,000	0.3	3	0.46
8	30.5–42.0	SM	19.6	18–26	34	0.5	44,000	0.3	4	0.44
9	42.0–60.0	SM	19.9	28–42	34	0.5	70,000	0.3	4	0.44

The findings of the MC model, i.e. predictions of ground surface settlement and wall deflection, are shown in Fig. 4; the projected outcomes are also compared to the observed outcomes. Figure 4 demonstrates that during first, second, and third stages of excavation, the wall deflections anticipated by the model are often larger than those observed in actual. This is due to the fact that the MC model disregards the small strain features and the high stiffness modulus behaviour of soil under low strain levels. It follows that the sands used in the MC model have a too-low Young's modulus, because the range of small strain soil area was higher in the beginning stages of excavation. In later excavation stages of excavation, i.e. fourth and fifth stages, predicted wall deflections are larger than field measurements at upper wall parts, but are comparable to actual measurements at lower wall parts. Both the field measurements and the predicted findings show that the greatest deflection occurs at the excavation level. However, the expected values are larger than what was actually measured in the field. One possible explanation could be that the MC model only uses one Young's modulus and does not distinguish between stiffness during loading and unloading. This occurs as a result of the MC model ignoring the behaviour of strain-dependent stiffness. Since the majority of the strains in the secondary influence zone (SIZ) are at low strain levels, the single Young's modulus used in the MC model was inaccurate.

4.2 HS Model

Table 6 provides the sand layer parameters for the HS model analysis. The predicted and observed ground surface settlements and wall deflections for the excavation by HS model are compared in Fig. 5. The findings of the HS model are significantly superior than those of the MC model, as shown in Fig. 5.

Thus, the HS model calculates the unloading stiffness. The HS model predicts that the largest ground surface settlement will occur between 0.6 and 1.0% of H_e away from the wall, with a value of approximately 0.47% of H_e. However, at the upper stages of excavation, the anticipated wall displacements are still more than the actual measurements. Settlements in the SIZ are still considered to be larger

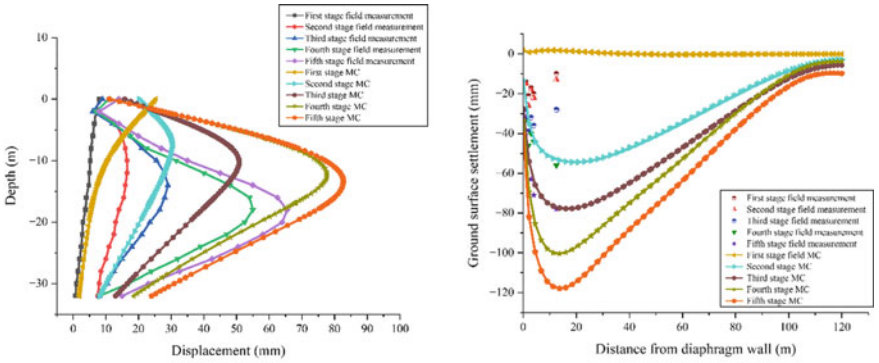

Fig. 4 Wall deflection and ground surface settlement by MC model

Table 6 Sandy soil parameters of HS model

Layer	Depth (m)	γ_t (kN/m^3)	N value	φ' (°)	c' (kPa)	ψ (°)	E_{50}^{ref}	E_{oed}^{ref}	E_{ur}^{ref}	K_0
2	2.0–6.5	20.9	5–11	32	0.5	2	9600	9600	28,800	0.47
4	8.0–17.0	20.6	5–17	32	0.5	2	13,200	13,200	39,600	0.47
5	17.0–23.5	18.6	5–17	32	0.5	2	13,200	13,200	39,600	0.47
6	23.5–28.5	19.6	5–17	33	0.5	3	13,200	13,200	39,600	0.46
8	30.5–42.0	19.6	18–26	34	0.5	4	26,400	26,400	79,200	0.44
9	42.0–60.0	19.9	28–42	34	0.5	4	42,000	42,000	126,000	0.44

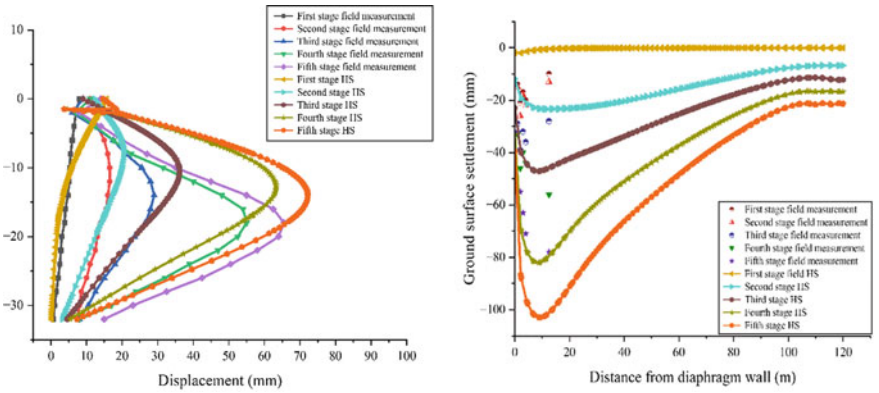

Fig. 5 Wall deflection and ground surface settlement by HS model

and wider than what was discovered in earlier studies. This is due to the fact that the HS model does not account for strain-dependent stiffness behaviour or small strain properties of soil. HS model are clearly superior to those of the MC model, as

shown in Fig. 5, particularly in terms of the prediction of surface settlements. The HS model calculates the unloading stiffness. The HS model predicts that the largest ground surface settlement will occur between 0.6 and 1.0% of $H_{e.}$

4.3 HSS Model

The results are displayed in Fig. 6, where $\gamma_{0.7}$ was considered as 10^{-4}. The required sand layer parameters used in the HSS model under analysis are displayed in Table 7.

Figure 6 compares and contrasts the surface settlements and wall deflections that occurred during excavation using the HSS model. Figure 6 illustrates how the HSS model significantly improves the MC model and the HS model in terms of ground surface settlements and wall deflections. The HSS model does not depict the significant wall toe displacements at later stages of excavation or the excessive wall deflection predictions at later stages of excavation. The greatest settlement in the HSS model is also around 0.6–1.0% of H_e from the wall and has a value of about 0.59% H_e, making it slightly smaller than the largest settlement in the HS model.

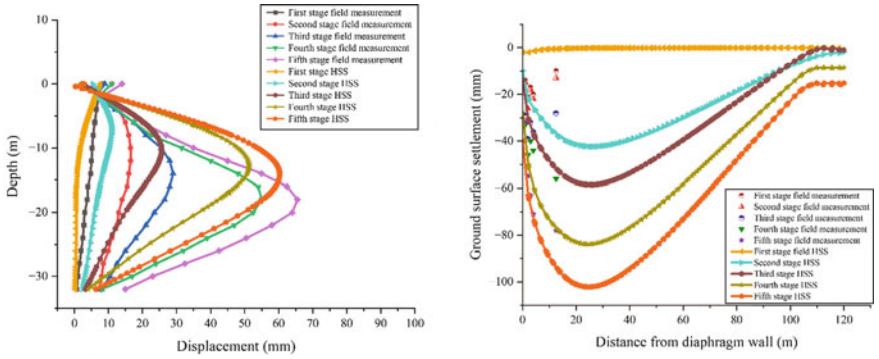

Fig. 6 Wall deflection and ground surface settlement by HSS model

Table 7 Sandy soil parameters of HSS model

Layer	Depth (m)	N value	V_s (m/s)	σ_3' (kPa)	G_0 (kPa)	G_0^{ref} (kPa)	$\gamma_{0.7}$
2	2.0–6.5	5–11	161	63	55,343	69,657	10^{-4}
4	8.0–17.0	5–17	183	150	69,974	57,153	10^{-4}
5	17.0–23.5	5–17	183	226	63,180	42,069	10^{-4}
6	23.5–28.5	5–17	183	278	66,577	39,966	10^{-4}
8	30.5–42.0	18–26	239	374	114,480	59,204	10^{-4}
9	42.0–60.0	28–42	287	518	167,115	73,412	10^{-4}

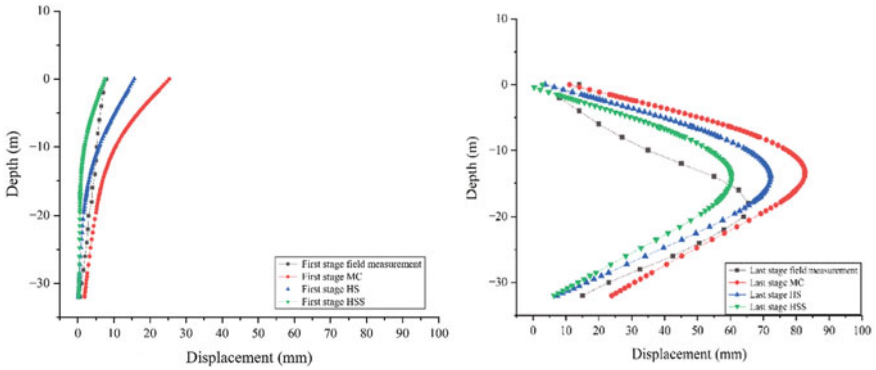

Fig. 7 Wall deflection at first stage and last stage by different models

4.4 Comparing of Results from Different Soil Models

Figure 7 depicts the comparison in the results of wall deflection between first and last stage of excavation by MC model, HS model, HSS model, and field observations; fourth stage wall deflection results by all models and field measurements are depicted by Fig. 8; in addition, results of ground surface settlement of last stage are also compared by different models, and field observations are depicted by Fig. 9. The anticipated wall deflections from both MC and HS models slightly surpass than the actual deflection. However, the projected wall deflections from the HSS model are reasonably equal to the field data during the first stage of excavation. The last stage results of HSS model are quite close to the actual results. However, the findings of HS model and MC model are overestimated as compared to actual data. All three models have surface settlements that are more than the fields observation data. While the settlement profiles of the HS and HSS models are more in line with field observations, those of the MC model are far off the mark.

4.5 Numerical Analysis in 3D

The numerical simulations are carried out in this section by using the geotechnical software PLAXIS 3D. In above subsection, study demonstrates that the best result was given by HSS model while contrasted to the MC and HS models. Consequently, in this section HSS model has been used for the analyses. According to Fig. 10, the study employed a finite element mesh with a total of 386,692 nodes and 268,067 elements.

Figure 11 compares and contrasts wall deflections that occurred during excavation using the HSS model in 2D and 3D analyses. It can be seen that the results from 3D are quite same below the excavation depth. In all stages, the wall deflection predicted by

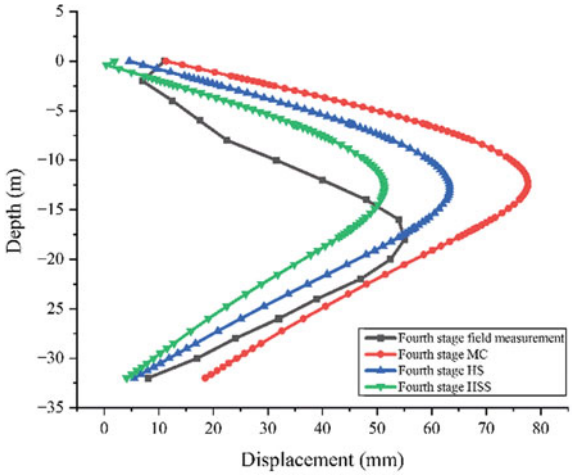

Fig. 8 Wall deflection at fourth stage by different models

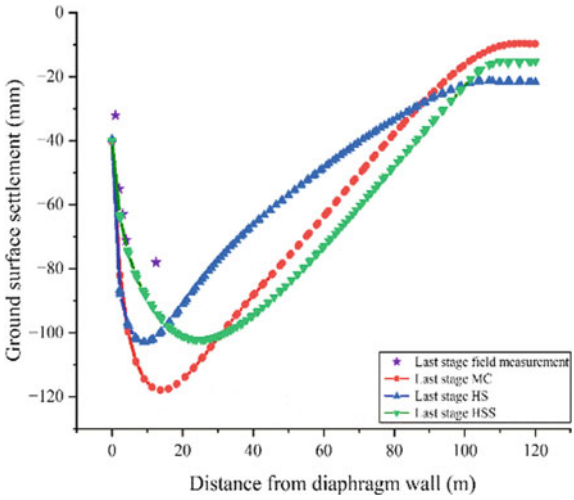

Fig. 9 Ground surface settlement at last stage by different models

3D analyses was slightly overestimated to some degree as compared to 2D analyses. However, it can be seen that the maximum value of deflection occurs at the same depth in twain 2D and 3D analysis, i.e. excavated depth. Lateral wall deflections calculated using 2D and 3D analysis are slightly underestimated and overestimated, respectively, when compared to actual wall deflections. However, predictions and actual outcomes have similar patterns.

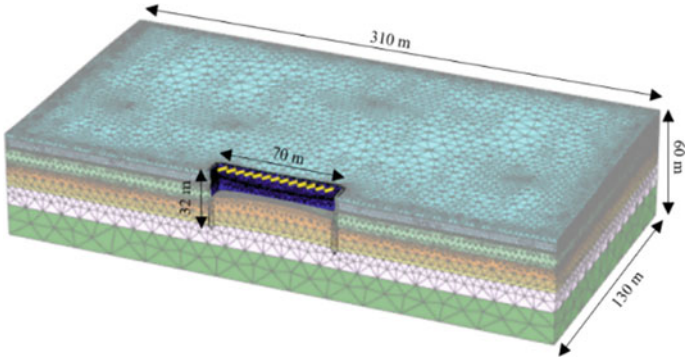

Fig. 10 Half mesh model from PLAXIS 3D

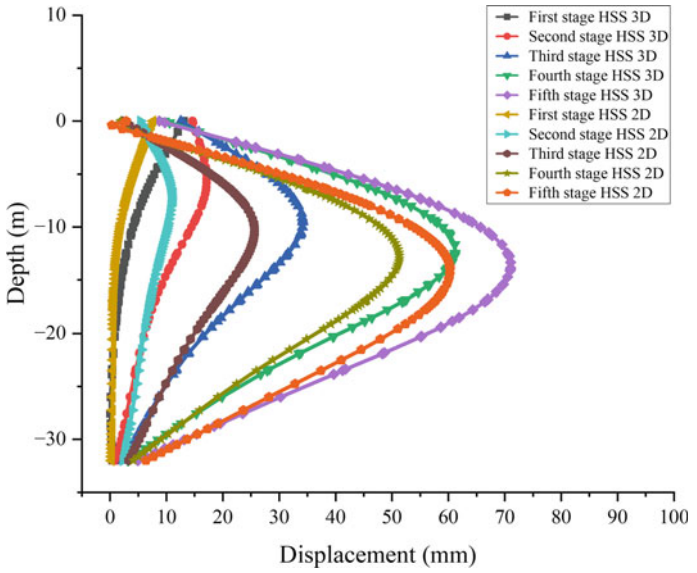

Fig. 11 Wall deflection by HSS model in 2D and 3D

5 Conclusion

- It has been found that using a more complex soil model in numerical computations leads to more accurate predictions of wall deflection and surface settlement, when compared to the HS model, which is better than the MC model, the HSS model is clearly the best option.
- The HSS model's predicted wall deflections are extremely similar to the actual field measurements, whereas those prediction by the MC and HS models are slightly bigger. The settlement profiles of the HS and HSS models are more in line with the field results than that of the MC model, which deviates by a large margin.
- In the case of a deep excavation in sand, the predictions for maximum wall deflection in both 2D and 3D modelling were found at the same depth approximately of each stage. However, the prediction by 3D model was slightly overestimated as compared to 2D model. So rather than 3D analysis, PLAXIS 2D analyses would be appropriate. Unlike 3D analyses, it doesn't require as much calculating time and is less tedious.

References

1. Hsiung B-CB (2009) A case study on the behaviour of a deep excavation in sand. Comput Geotech 36(4):665–675. https://doi.org/10.1016/j.compgeo.2008.10.003
2. Ou C-Y, Hsieh P-G, Chiou D-C (1993) Characteristics of ground surface settlement during excavation. Can Geotech J 30(5):758–767. https://doi.org/10.1139/t93-068
3. Ou C-Y (2006) Deep excavation: theory and practices. Taylor Francis, Netherlands
4. Lim A, Ou C-Y, Hsieh P-G (2010) Evaluation of clay constitutive models for analysis of deep excavation under undrained condition. J Geoeng 5(1):9–20
5. Khoiri M, Ou C-Y (2013) Evaluation of deformation parameter for deep excavation in sand through case histories. Comput Geotech 47:57–67. https://doi.org/10.1016/j.compgeo.2012.06.009
6. Hsieh P-G, Ou C-Y (1998) Shape of ground surface settlement profiles caused by excavation. Can Geotech J 35(6):1004–1017. https://doi.org/10.1139/t98-056
7. Pakbaz MS, Imanzadeh S, Bagherinia KH (2013) Characteristics of diaphragm wall lateral deformations and ground surface settlements: case study in Iran-Ahwaz metro. Tunn Undergr Sp Technol 35:109–121. https://doi.org/10.1016/j.tust.2012.12.008
8. Long M (2001) Database for retaining wall and ground movements due to deep excavations. J Geotech Geoenviron Eng 127(3):203–224. https://doi.org/10.1061/(ASCE)1090-0241(2001)127:3(203)
9. Aswathy MS, Vinoth M, Mittal A, Behera S (2020) Prediction of surface settlement due to deep excavation in indo-gangetic plain: a case study. Indian Geotech J 50(4):620–633. https://doi.org/10.1007/s40098-019-00399-x
10. Ou C-Y, Shiau B-Y, Wang I-W (2000) Three-dimensional deformation behavior of the Taipei National Enterprise Center (TNEC) excavation case history. Can Geotech J 37(2):438–448. https://doi.org/10.1139/t00-018
11. Calvello M, Finno RJ (2004) Selecting parameters to optimize in model calibration by inverse analysis. Comput Geotech 31(5):410–424. https://doi.org/10.1016/j.compgeo.2004.03.004

12. Nikolinakou MA, Whittle AJ, Savidis S, Schran U (2011) Prediction and interpretation of the performance of a deep excavation in Berlin sand. J Geotech Geoenviron Eng 137(11):1047–1061. https://doi.org/10.1061/(ASCE)GT.1943-5606.0000518
13. Ou C-Y, Lai C-H (1994) Finite-element analysis of deep excavation in layered sandy and clayey soil deposits. Can Geotech J 31(2):204–214. https://doi.org/10.1139/t94-026
14. Hsiung B-CB, Dao S-D (2014) Evaluation of constitutive soil models for predicting movements caused by a deep excavation in sands. Electron J Geotech Eng 19:17325–17344
15. Likitlersuang S, Surarak C, Wanatowski D, Oh E, Balasubramaniam A (2013) Finite element analysis of a deep excavation: a case study from the Bangkok MRT. Soils Found 53(5):756–773. https://doi.org/10.1016/j.sandf.2013.08.013
16. Bolton MD (1986) The strength and dilatancy of sands. Geotech 36:65–78
17. Schmertmann JH (1970) Static cone to compute static settlement over sand. J Soil Mech Found Div 96(3):1011–1043. https://doi.org/10.1061/JSFEAQ.0001418
18. Schanz T, Vermeer PA, Bonnier PG (1999) The hardening soil model: Formulation and verification. Beyond 2000 Comput Geotech 10 Years PLAXIS. Balkema, Rotterdam
19. Hardin BO, Drnevich VP (1972) Shear modulus and damping in soils: design equations and curves. J Soil Mech Found Div 98(7):667–692. https://doi.org/10.1061/JSFEAQ.0001760